Massive Enhancement of Photoluminescence through Nanofilm Dewetting

Peiwei Lee,[†] Wei-Cheng Li,[†] Bin-Jih Chen,[†] Chih-Wei Yang,[†] Chun-Chih Chang,[†] Ioan Botiz,[‡] Günter Reiter,[‡] Tsang-Lang Lin,[§] Jau Tang,[⊥] and Arnold Chang-Mou Yang[†,*]

[†]Department of Materials Science and Engineering, National Tsing Hua University, Hsinchu, Taiwan, [‡]Institute of Physics and Freiburg Institute for Advanced Studies, Albert-Ludwigs-Universität, Freiburg, Germany, [§]Department of Engineering and Systems Science, National Tsing Hua University, Hsinchu, Taiwan, and [⊥]Research Center for Applied Sciences, Academia Sinica, Taipei, Taiwan

ABSTRACT Due to the rather low efficiencies of conjugated polymers in solid films, their successful applications are scarce. However, recently several experiments indicated that a proper control of molecular conformations and stresses acting on the polymers may provide constructive ways to boost efficiency. Here, we report an amazingly large enhancement of photoluminescence as a consequence of strong shear forces acting on the polymer chains during nanofilm dewetting. Such sheared chains exhibited an emission probability many times higher than the nonsheared chains within a nondewetted film. This increase in emission probability was accompanied by the emergence of an additional blue-shifted emission peak, suggesting reductions in conjugation length induced by the dewetting-driven mass redistribution. Intriguingly, exciton quenching on narrow-band-gap substrates was also reduced, indicating suppression of vibronic interactions of excitons. Dewetting and related shearing processes resulting in enhanced photoluminescence efficiency are compatible with existing fabrication methods of polymer-based diodes and solar cells.

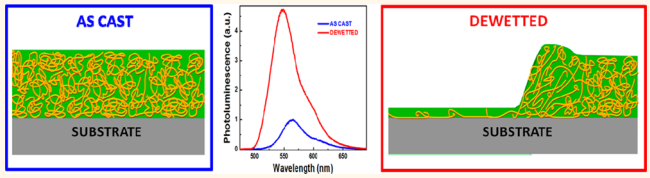

KEYWORDS: conjugated polymers · dewetting · photoluminescence · optoelectronic efficiency · stress effects · electron–phonon interactions

Thin films of conjugated polymers (CPs) have attracted widespread interest, owing to low-cost processing possibilities, their unique mechanical properties, and tunable optoelectronic behavior that make them highly appealing for lighting, energy harvesting, and microelectronics.[1−5] However, electronic states excited by photon absorption[6−12] are affected by self-trapping and subsequent nonradiative processes,[13] resulting often in a low photoluminescence (PL) quantum efficiency of CPs.[14] The strong coupling of the excited states to the phonon spectrum[1,2,6,9−12] prevails in the chain-like molecules that are intrinsically softer than inorganic crystalline materials. It occurs as the time-integrated chain vibrations, swayed by the local electric fields induced by the excited states, causes local deformations of the molecular strands and, in turn, may block coherent energy or charge transport. Such molecular deformations usually lead to exciton entrapment and obstruction of the radiative pathways. In addition, ordered domains and conformational changes of the polymers[15−20] that arise due to environmental factors, *e.g.*, temperature variation[21,22] or solvent exposure,[23,24] strongly influence opto-electronic properties of CPs.

For amorphous dry films, the strong vibronic coupling, however, may be suppressed by putting the polymer strands under a tension.[7,25−27] Recently, dramatic enhancement of PL efficiency was reported in isolated molecules of poly[2-methoxy-5-((2′-ethylhexyl)oxy)-1,4-phenylenvinylene] (MEH-PPV) dispersed in the solid films of polystyrene when they were substantially stretched.[7] Similar results were also obtained for the cyrstallizable CP of poly(3-hexylthiophene).[28] This, consistent with the electron–phonon coupling mechanism, suggests that optoelectronic behavior in this class of materials can be modified or even controlled by mechanical deformations and stresses.[25] Thus, one may expect substantial variations in how the exciton

* Address correspondence to acyang@mse.nthu.edu.tw.

Received for review February 25, 2013 and accepted July 26, 2013.

Published online July 27, 2013
10.1021/nn4009752

forms, moves, and annihilates when conjugated polymers are put under a mechanical tension.

Such a mechanical effect is expected to reign even in liquid CP solutions. But there, the presence of solvent alters and sometimes even dominates the energy transfer pathways. Notably, energy transfer is reduced between CP molecules. Moreover, arising from solvent plasticization that leads to critical lowering of the Young's modulus and thus decreased mechanical work, exciton trapping *via* local mechanical deformations[12] plunges. Consequently, self-trapping of exciton dwindles, as evidenced by a less blinking and slower photobleaching behavior of the dissolved molecules.[29,30] In addition, in a liquid solution segmental mobility may vary widely even within a single molecule due to specific segmental interactions such as partial adsorption. The notion of "mean chain conformations" that often refers to the global ensemble average of segmental distribution of the entire molecule is no longer suitable for describing the molecular stress state of the CP molecules. Rather, the focus has to be on the local behavior of chain segments influenced by mechanical stresses.[29,30] Likewise, for films of CPs annealed in solvent vapor, exciton trapping is expected to decline in the solvated state due to the presence of the solvent. However, when these so annealed films are returned back to the dry state, optoelectronic efficiency will decrease due to enhanced mechanical interactions.[24]

For various optoelectronic applications, conjugated polymers are packed into solid films of small thicknesses,[31,32] sometimes even less than the characteristic size of such molecules, *i.e.*, their radius of gyration (R_g). Often significant residual stresses are generated by the processes involved in film formation.[33−35] For example, by spin-coating, during which solvent evaporates rapidly within a few seconds, the giant polymer molecules are quickly transformed from isolated fully solvated molecules to dry aggregates consisting of densely packed, but usually not equilibrated polymers confined in the thin solid film. Interactions with the substrate and the free surface during solvent evaporation also strongly influence molecular packing and the molecular stress state. Consequently, one may anticipate that, based on the effects of molecular stresses and conformations, PL varyies with film thickness (h) as the fractions of the MEH-PPV chains in contact with the substrate and the free surface alter.

RESULTS AND DISCUSSIONS

As shown in Figure 1, PL of as-prepared thin films of pure MEH-PPV showed a clear thickness dependence, but also depended on the type of substrate used. The general trend of increasing PL with decreasing h shown in Figure 1 is related to the effect of residual stresses[33−35] from the highly nonequilibrated polymer molecules in the solid films. Since in such thin films residual stress increased as film thickness decreased,[36,37] the data of Figure 1 suggests that higher stresses acting in thinner

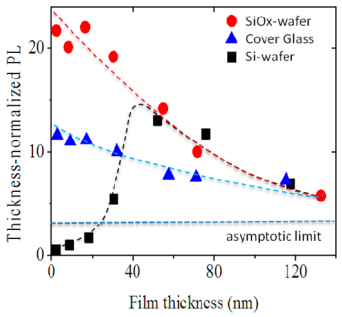

Figure 1. Thickness-normalized PL peak intensity *versus* film thickness of pristine 100% MEH-PPV films on different substrates: Si wafer (bare Si wafer with a native oxide of ~2 nm), SiOx−wafer, and cover glass. The broken lines are drawn to guide the eye. The dotted line indicates the asymptotic limit of PL for infinitely thick films where residual stresses have diminished.[36,37]

films gave rise to an increased PL efficiency. This hypothesis is consistent with previously reported stretching experiments.[7] The higher PL efficiencies of the films on SiOx wafer (Si wafers with a thick oxide layer of ~500 nm) with respect to those on cover glass may be related to differences in adsorption strength and molecular packing, as suggested by X-ray reflectivity measurements (see Experimental Section and Supporting Information). In contrast, on Si wafers which have a narrow energy gap (E_g = 1.12 eV compared to E_g > *ca.* 2 eV for MEH-PPV)[12] PL started to diminish for h smaller than *ca.* 50 nm. This effect arose from the quenching effect operative for films thinner than approximately the exciton diffusion length,[38,39] acting on the photoinduced excitons migrating near the film/Si−wafer interface, where a large electric field arising from Fermi-level alignment[12] tore the excitons apart and annihilated them.[23] For substrates with band gaps greater than that of the conjugated polymer, *e.g.*, cover glass and SiOx−wafer, such effects did not exist because the electric fields acting at the heterojunction were not dissociative for the excitons.[12]

One expects that the increase of PL with decreasing h on SiOx wafer or cover glass inherited from film preparation would disappear once the polymers are equilibrated. This could be achieved by annealing the films above the glass transition temperature, either by heating them or by exposing them to solvent vapor.[23−26,38−40] However, in our system, dewetting took place when such films became liquid. During the dewetting process, polymers were moved over long distances by the capillary force and the residual stresses (see Figure 2a). Ultimately, these sheared polymers were deposited in droplets or remained as a residual layer adsorbed on the substrate (see Figure 2b). In order to explore the impact of dewetting on optoelectronic properties, we measured photoluminescence in parallel with dewetting.

When films of pure MEH-PPV, or blended with low molecular weight polystyrene (PS), were annealed at temperatures above *ca.* 100 °C, dewetting started after

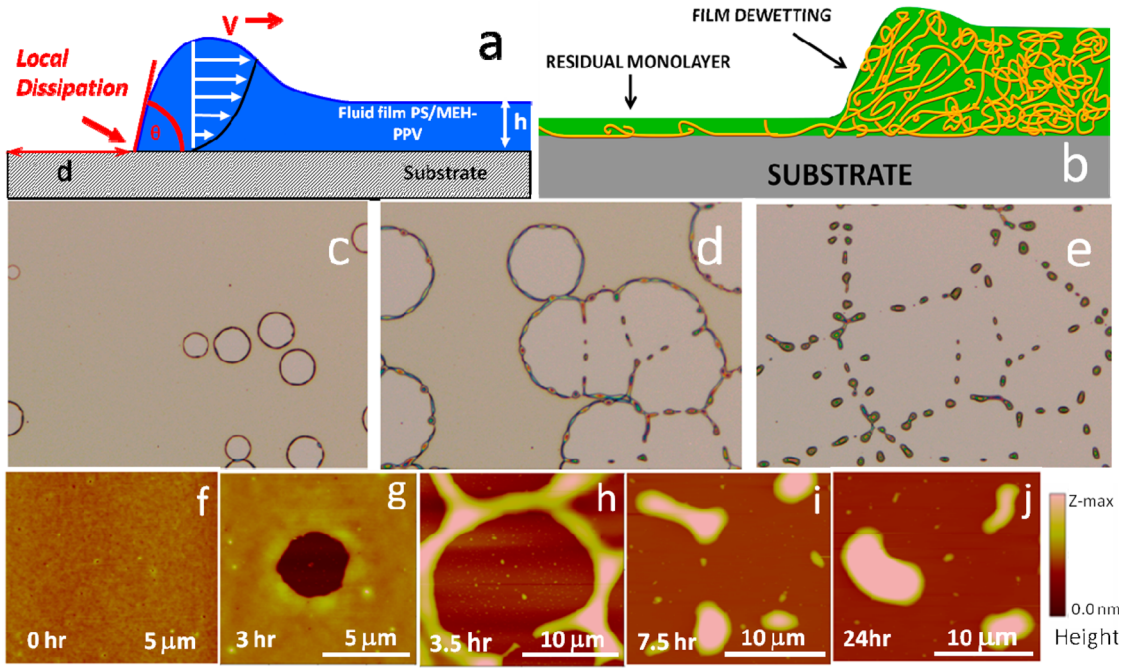

Figure 2. (a) Schematic depiction of the dewetting process, with *d*, *V*, and θ being the dewetted distance, the dewetting velocity, and the contact angle, respectively. (b) Schematic drawing indicating the stretching of polymer by dewetting and the formation of a residual layer that has been left behind by the moving dewetting front. (c–e) Optical micrographs depicting dewetting of a 40 nm thick MEH-PPV/PS film (*c* = 15 wt %) after 1, 2, and 25 min, respectively. Size of images is 286 × 212 μm^2. Film dewetted at 135 °C in an inert nitrogen atmosphere on a silicon wafer coated with a thin layer of polydimethylsiloxane (PDMS). (f–j) AFM micrographs of height topography depicting the dewetting sequence for 20 nm thick MEH-PPV/PS films (*c* = 15 wt %) on bare Si wafer; z_{max} = 50 nm (for f, g) or 300 nm (for h–j).

an incubation time through the growth of small pinholes (Figure 2g), which grew in size (Figure 2c) and later on coalesced (Figure 2d and h), leading to the formation of droplets (Figure 2e, i, and f). The required annealing times for initiating and completing dewetting increased significantly with film thicknesses (*h*) and concentration (*c*) of MEH-PPV in a PS matrix. For films below $h \approx 10$ nm on PDMS-coated substrates, where the PDMS layer was introduced for facilitating dewetting (please also see the Experimental Section), the instability was probably driven by spinodal dewetting,[42] as no obvious incubation time was required for pinhole formation.

In the process of dewetting, a residual layer of adsorbed polymers was "exposed" on the substrate (see Figure 2b). The thickness of this residual layer, measured by X-ray reflectivity[43] using synchrotron radiation as well as AFM topographic analysis on scratched samples, was found to be *ca.* 2–3 nm, almost independent of *h* and slightly increasing with *c*. The existence of the residual layer reflects the anchoring of polymers on the substrate. Forced by the flow field generated by the dewetting front, chains were expected to be preferentially oriented in the direction of the movement of the dewetting front similar to "molecular combing" of DNA.[44] Most likely, these "combed polymers" were also stretched within the receding meniscus exerted by the capillary forces. Finally, when deposited in droplets and the residual monolayer, polymer may initially still exhibit nonequilibrium chain conformations and an altered entanglement structure due to the previous shearing process in the course of dewetting. The droplets formed during the final stage of dewetting had, depending on *h* and substrate properties, a height up to several hundred nanometers and a lateral extension of some tens of micrometers. These droplets, which had a contact angle ranging from approximately 5° to 10°, could be removed when washing the films in a good solvent. However, the residual layer remained, illustrating the large difference in substrate adhesion of droplets and residual layer.

During dewetting, the PL of the films underwent dramatic changes, as can be seen in Figure 3a and b. During the initial incubation period, the still intact films manifested a significant decrease of PL intensity along with a red shift (from 565 to 585 nm for the 20 nm MEH-PPV/PS films, Figure 3b). The data indicate that, before the onset of dewetting, (partial) stress relaxation was induced by annealing, during which some chain aggregation was occurring as hinted by the decrease of PL (see Figure 3a and b)[7] in conjunction with the red shift probably caused by an increase of conjugation length. Although the stress reduction was significant, *e.g.*, as manifested by the 20 nm films for 30 min annealing on a glass substrate (Figure 3a and Figure 1), the capillary force, arising from the long-range van der Waals interactions between the free surface and the film/substrate interfaces,[40–42] was unchanged since the

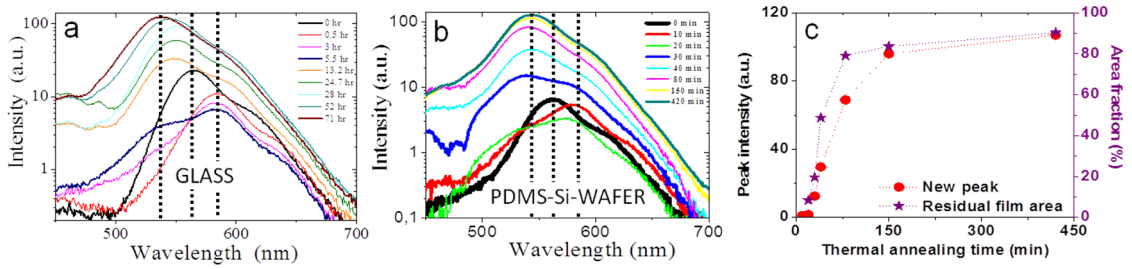

Figure 3. Temporal evolution of the emission spectra for 20 nm thick films obtained during dewetting on (a) cover glass (MEH-PPV/PS; *c* = 15 wt %) and (b) PDMS-coated Si wafer (MEH-PPV/PS; *c* = 25 wt %). (c) PL emission intensity of the emerging new peak and fraction of dewetted area *versus* dewetting time for the 20 nm MEH-PPV/PS films in (b).

film thickness was approximately constant during this period of annealing. Thus, due to the substantial and continuous relaxation of the residual stresses prior to the onset of dewetting, the molecular flows that created the residual layer and droplets were driven by polymer transport moving from the regions of lower heights to that of greater heights in order to minimize the capillary interactions. As evident from the considerable increase of dewetted surface area, polymer chains are in motion over distances many times their molecular dimension, not only in the region of the residual layer but also in the droplets, and are stretched by the acting frictional forces during this flow process. Hence, the existence of stretched chains in the droplets, particularly in the upper portion of the droplet, is clear.

Once dewetting started, a new PL peak appeared at a wavelength blue-shifted relative to the original emission peak. Within a small uncertainty on the order of 1−4 nm arising from the use of multiple samples in each annealing series (Experimental Section), the position of this new peak (*ca.* 543 nm for 20 nm thick 15% MEH-PPV/PS films) remained approximately constant throughout the whole dewetting process. Its intensity, on the contrary, increased by more than a factor of 10 (for h = 10 nm on silicon wafer). As can be clearly seen in Figure 3c, the increase in PL followed the increase in dewetted area with annealing time. As stated before, since the residual stress diminished rather quickly upon annealing, the driving forces for dewetting as well as the observed enhanced PL may be dominated by the actions of the capillary forces. Obviously, the polymer chains are stretched into flows under tension of this capillary force, as well as the remaining component of the decaying residual stress.

Generally, due to the plasticizing effect of the low molecular weight polystyrene, the blend films dewetted faster than pure MEH-PPV films. In addition, an even stronger enhancement of PL compared to pristine MEH-PPV films was observed. Separate experiments of dewetting triggered by exposing the films to solvent vapor (solvent annealing) (not shown) produced almost identical results, clearly indicating that the new PL peak was not arising from thermal degradation but from chain movements and deformations during dewetting. The exact wavelengths of the red-shifted peak and the blue-shifted peak depended on c, h, and substrate interactions. In contrast to the red-shift observed for annealed but not yet dewetted films, the blue shift of PL during dewetting indicates a decrease of conjugation length of the MEH-PPV molecules that were dragged over long distances during dewetting. Probably, in the break-up of the dewetting films, polymer chains underwent changes in conformational states and alteration in intersegmental chain entanglements resulting in a reduction of conjugation length.

To gain further insight, PL spectra before annealing were analyzed by Gaussian curve fitting. We obtained for the peak positions of the emissions dominated by intrachain and interchain interactions wavelengths of 565 and 595 nm, respectively, in good agreement with those reported elsewhere.[37] The spectra during dewetting were analyzed by assuming unchanged wavelengths for these two emission peaks and adding a third peak for the additional contribution at 543 nm (for 20 nm films). Evidently, in the course of dewetting the intensity of the new peak rapidly increased, while the original emission peaks increased only modestly. Qualitatively, the same behavior was observed for all film thicknesses.

The influence of film thickness and film−substrate interactions on the evolution of the PL intensities during dewetting is illustrated in Figure 4a, b, and c, respectively. We present the PL enhancement factor, defined as PL in the course of annealing divided by PL before annealing. The period before the onset of dewetting, during which relaxations in the film were able to reduce PL, was shortened when decreasing film thickness. For the thinnest films of h = 10 nm, only an increase of PL could be detected. Thus, upon decreasing the film thickness, the reduction of the incubation time prior to dewetting and the enhanced molecular stresses driving the dewetting (the recoiling residual stresses and the capillary forces)[33−37,40−42] caused an almost instantaneous generation of a blue-shifted peak and a strong enhancement of PL intensity.

In contrast to an initial reduction in PL before dewetting, PL increased as soon as dewetting started. There, the PL enhancement factor was larger the thinner the films were. Here, the strong influence of the substrate on PL properties of polymer films has to

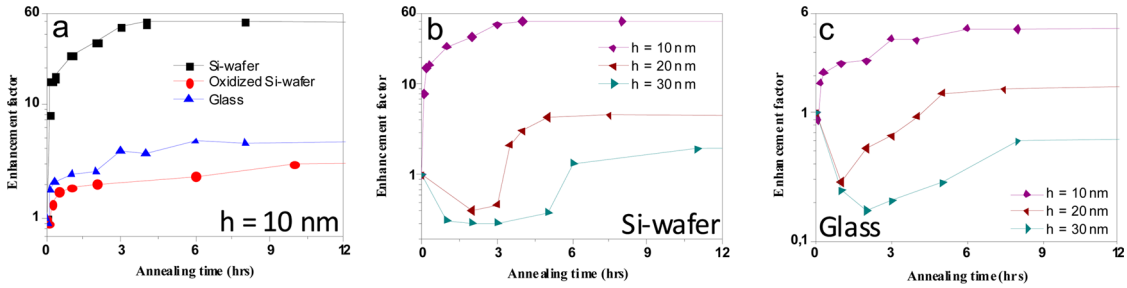

Figure 4. Temporal evolution of the PL enhancement factor for films (c = 15 wt %) in the course of annealing and dewetting: (a) for different substrates (h = 10 nm): Si wafer, SiOx wafer, and cover glass; for various thicknesses on (b) Si wafer and (c) cover glass.

be emphasized. For nondewetted films thinner than 50 nm on Si wafers, exciton quenching was responsible for the low PL intensities of the as-prepared films (see Figure 1). From Figure 3a and b, it is clear that upon dewetting PL for such thin films on Si wafers increased drastically. Interestingly, close to nonquenching interfaces (cover glass and SiOx wafers) dewetting also induced an increase of PL intensity, but of a significantly smaller magnitude, *e.g.*, 50-fold (on Si wafer, Figure 4b) *versus* 5-fold (on cover glass, Figure 4c) for h = 10 nm. Intriguingly, the PL intensities of the fully dewetted samples were approximately independent of the choice of the substrate (see later). Obviously, in addition to the effects by the stresses induced by dewetting on the molecular strands of MEH-PPV, the resulting changes in local film thickness in droplets can be larger than the exciton diffusion length and thus were able to reduce the exciton quenching effect. Consequently, the much stronger enhancement of PL observed for films on Si wafers was the result of a dewetting-induced stress acting on the polymers in combination with a reduction of the heterojunction quenching effect due to the local increase of thicknesses in the droplets.

For thicker films, the dewetting-induced enhancement was not always able to compensate for the initial reduction in PL attributed to thermally induced relaxations of residual stresses. In a partially dewetted film, PL from the dewetted regions was, however, always significantly greater than PL from the annealed but not yet dewetted regions of the film. By the same token, the shifting of the dewetting-induced PL peak toward the blue part of the light spectrum was generally more pronounced the thinner the films were. For example, this peak emerged at *ca.* 552 nm for h = 30 nm, *ca.* 547 nm for h = 20 nm, and *ca.* 536 nm for h = 10 nm (for c = 25% MEH-PPV/PS films on bare Si wafer). The increase of the blue shifts in the thinner films replicated the more pronounced changes in molecular conformations arising from the greater capillary forces and the residual stresses operative in the thinner films during dewetting. In Table 1 we give a brief summary of the PL enhancements and blue shifts for films (c = 15 wt % MEH-PPV/PS) of different thicknesses dewetting on various substrates. The molecular changes that are attributed to the decrease of conjugation length were most likely dominated by the creation of conjugation-disruptive "molecular kinks" near the stretched chain entanglements. As detailed separately for solvent-induced dewetting (*i.e.*, by solvent annealing), the blue shift eventually reduced in magnitude at longer dewetting times, indicating the ultimate relaxation of these molecular kinks. The small final blue shift of the thinnest films (10 nm) dewetting on a SiOx wafer (Table 1) can be tentatively attributed to the short dewetting distances possible between neighboring dewetting holes, a consequence of an extremely high nucleation density of dewetting holes. In addition, part of the blue shift may have been recovered by a relaxation process similar to that observed in samples of solvent dewetting.

As mentioned above, PL of fully dewetted films was found to be independent of the substrate properties. In order to identify the origin of this observation, we measured PL from various regions of the dewetted films using a confocal setup coupled with an AFM for precision positioning that allowed spectroscopically determining the PL with a spot size of about 1 μm^2. We compared PL spectra obtained from the as-cast film with spectra obtained from dewetted droplets, the residual layer remaining in the dewetted areas, and the still intact parts of the film that had undergone some annealing and thus contained relaxed polymers (Figure 5a). The corresponding spectra for these regions exhibited characteristic positions of the PL peaks and thus represent reliable fingerprints of the respective contributors to the investigated PL enhancements. The intensities, however, were used with caution, as they sensitivly depended on the surface curvature of the surveyed spots. Therefore, only planar objects, such as films or residual layers, were compared for the intensities.

The decrease of PL emission and the associated red shifts in the stress-relaxed films before the onset of dewetting, observed by using a PL spectrometer that averaged over the whole sample (see Figure 3), were replicated by using micro-PL on the intact (nondewetted) parts of the film (Figure 5a). Surprisingly, the 20 nm

TABLE 1. Final PL Enhancement Factors (ξ) and Blue Shifts ($\Delta\lambda$) for MEH-PPV/PS Films (c = 15%) of Different Thicknesses Dewetting on the Various Substrates[a]

	τ = 10 nm	τ = 20 nm	τ = 30 nm
Si wafer	ξ = 48.8 fold;	ξ = 5.2 fold;	ξ = 2.5 fold;
	$\Delta\lambda$ = 37 nm (573 → 536 nm)	$\Delta\lambda$ = 15 nm (562 → 547 nm)	$\Delta\lambda$ = 10 nm (562 → 552 nm)
SiO_x wafer	ξ = 3.0 fold;	ξ = 1.2 fold;	ξ = 0.6 fold;
	$\Delta\lambda$ = 16 nm (556 → 540 nm)	$\Delta\lambda$ = 15 nm (560 → 545 nm)	$\Delta\lambda$ = 14 nm (564 → 550 nm)
cover glass	ξ = 4.9 fold;	ξ = 1.8 fold;	ξ = 0.7 fold;
	$\Delta\lambda$ = 31 nm (571 → 540 nm)	$\Delta\lambda$ = 16 nm (564 → 548 nm)	$\Delta\lambda$ = 14 nm (565 → 551 nm)

[a] Raw data in Figure S4, Supporting Information. For the final peak positions of the dewetting samples, an uncertainty of ~1-4 nm existed mainly arising from the use of multiple samples for each annealing series (please see Experimental Section).

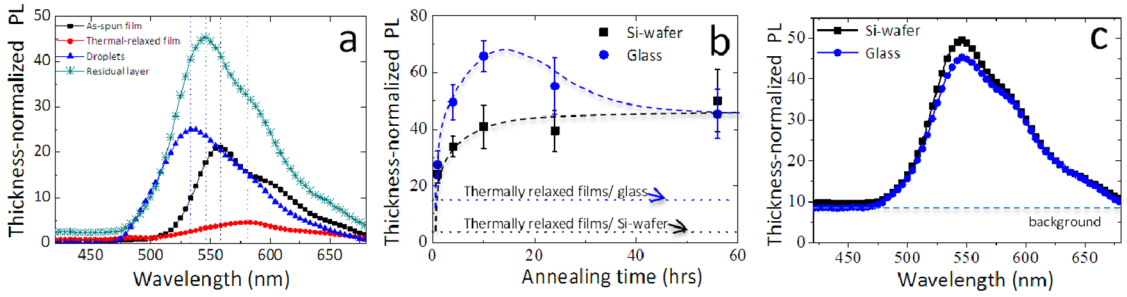

Figure 5. (a) Local PL spectra from a thin film (c = 15%, h = 20 nm) before and after dewetting on a Si wafer. (b) Temporal variation with annealing time of the PL intensities from residual layers on a Si wafer and cover glass, respectively. A fixed value of 2 nm was used for the thickness of the residual layer. (c) PL spectra from residual layers of fully dewetted films on a Si wafer and cover glass, respectively.

thermally relaxed but nondewetted film emitted, normalized by thickness, an about 10-fold lower amount of photons than the 2 nm thin layer remaining after dewetting. Consistently, a cross-sectional PL mapping over the partially dewetted films using a scanning near-field optical microscope protrayed a substantial PL increase within the hole regions relative to that outside (not shown). Owing to the significantly easier operation and finer spectral resolution, local optical properties of the film were obtained mostly by using the confocal micro-PL, however. The spectra from both the residual layer as well as the droplets exhibited a clear blue shift of the peaks, being larger for PL from droplets. Thus, when integrating PL over the whole sample, the emerging new peak (Figure 3) came from both the residual layer and the droplets, suggesting that large molecular deformations had taken place in both the residual layer and the droplets.

The local PL efficiency (defined as the peak PL intensity normalized by the local thickness) of the residual layer was found to increase rapidly with the onset of dewetting (Figure 5b). Interestingly, exciton quenching was already switched off in the residual layer on silicon at an early stage of dewetting, as seen from the increased PL intensity relative to that of the as-spun film on cover glass (Figure 5b). It is important to note that the PL spectra from the approximately equally thick residual layers on glass and Si wafers were almost identical (Figure 5c). The absence of exciton quenching indicated that charge recombination was extremely efficient in these about 2 nm thick layers. Evidently, our experiments indicate that a state of molecular stress may dramatically alter the formation and properties of excitons.

We attribute the extraordinarily large optoelectronic enhancement to effective changes in the molecular stress states resulting from shear flows induced by nanofilm dewetting. When conjugated polymer chains are stretched, self-trapping of excited electronic states is significantly depressed due to increased difficulties to accumulate local deformations for exciton entrapment, yielding a much more efficient charge recombination. This enhancement of PL came along with the formation of a new emission peak, emerging at a wavelength blue-shifted relative to the emission of initial film, which signifies extensive molecular changes of the CP chains stretched during dewetting. We emphasize that dewetting did not change the total number of illuminated molecules. Thus, the increase in PL has to be attributed to a more efficient emission per molecule. A similar stress-induced enhancement of the optoelectronic efficiencies was observed in uniaxially stretched films containing conjugated polymers.[7] We suggest that the deformation-induced changes in the molecular stress states led to a reduced phonon−exciton coupling of molecularly strained conjugated polymer chains. The PL enhancement due to the stress-rigidified effect under the molecular flows is consistent with the widely reported effects of increased chain rigidity *via* chemical routes such as covalent incorporation of the

bulky side chains,[45] macrocycles,[46] or cyclodextrin rings.[47] To be reported separately,[22] the time-resolved PL of stretched CP strands illustrates significantly lesser temperature dependence, revealing the suppressed exciton–phonon coupling by molecular stresses.

Spatially resolved micro-PL spectroscopy revealed that such strained polymer chains existed in both the droplets and the thin residual layers on the "exposed" substrate, but only to a much lower level in the nondewetted regions of the films. Intriguingly, these strained chains within the 2 nm thin residual layer displayed almost no exciton quenching, even when they were adsorbed at a highly dissociative interface. This indicates that formation, fine structures, and properties of excitons in conjugated polymers may be altered and controlled through appropriate management of the molecular stress states. Preliminary single-molecule spectroscopy on thin PS films containing very dilute MEH-PPV ($c < 10^{-9}$ g/cm^3) indicated that the CP strands stretched in the residual monolayer blinked significantly less with brighter PL emissions that decayed considerably slower, in line with the molecular stress effects observed and reported here. All these findings support the view that, due to a weaker electron–phonon coupling, energy dissipation in constrained polymers can be substantially reduced. Thus, deforming polymers, through dewetting or similar processes, can induce a large enhancement of optoelectronic properties in thin films, which may find useful applications in energy conversion and lighting devices. The here employed processes of thin film preparation and annealing are fully compatible with current prevailing technology for microelectronics and display industries and thus may allow generating efficient optoelectronic devices based on conjugated polymers.

CONCLUSIONS

In summary, large increases of PL efficiency were observed in the CP nanofilms dewetted on various substrates when annealed at an elevated temperature. The PL increases were attributed to the effect of tensile molecular stresses acting on the CP segments resulting mostly from the capillary force acting in the film during dewetting. Stretching the entangling CP molecules introduced variations of the molecular environment of the CP chains and produced a reduction of the effective conjugation lengths, causing a PL blue shift, most likely *via* the formation of molecular kinks near the stretching points between entangling chains. Furthermore, during the initial annealing stage before the onset of dewetting, pronounced decreases of emission intensity accompanied by red shifts were observed, revealing the relaxation of the residual stress and simultaneous molecular aggregation that gave rise to an increase of conjugation length. In addition, exciton quenching, which normally takes place at the heterojunctions between CPs and low-band-gap substrates, diminished when the CP molecular chains were stretched under large molecular stresses, indicating that the molecular stresses may strongly influence the formation and properties of the excitons. Finally, the methods of dewetting and related molecular shearing are compatible with existing microelectronic fabrication processes and thus may be useful for the development of polymer-based diodes and solar cells.

EXPERIMENTAL SECTION

Sample Preparation and Dewetting. The conjugated polymer used here, poly[2-methoxy-5-((2′-ethylhexyl)oxy)-1,4-phenylenevinylene], MEH-PPV, was purchased from Sigma-Aldrich Chemical Co., with a molecular weight (M_w) of *ca.* 250 000 g/mol and with a polydispersity (M_w/M_n) around 5. In order to enhance the dewetting process, MEH-PPV was blended with low molecular weight polystyrene, bought from Pressure Chemical Co., with a molecular weight of $M_w = 2$ kg/mol and $M_w/M_n \leq 1.06$. A solvent mixture of equal parts toluene (HPLC/SPECTRO, Tedia), tetrahydrofuran (THF, anhydrous, Tedia), and cyclohexanone (GC grade, Sigma-Aldrich) was used to make the polymer solutions used for preparing the film samples. Thin films of pure MEH-PPV and of MEH-PPV/PS blends with an MEH-PPV fraction (c) between 0 and 25% were prepared for the experiments. The polymer solutions were stirred slowly at 50 °C for 12–24 h, filtered (0.45 μm pore size) to remove any nondissolving particles, and then spin-casted on a 1 cm × 1 cm substrate, resulting in smooth and uniform films. By adjusting the spin-speed, the film thickness (h) was controlled in the range from 10 to 60 nm.

Several different substrates were employed. Bare silicon wafers with a thin native oxide layer of about 2 nm (Si wafer) were used. In certain experiments, where dewetting was to be facilitated, a thin layer of polydimethylsiloxane (Sylgard 182, Dow Corning) was coated, by spin coating and then cured at 130 °C, on the silicon wafer before depositing the polymer film. The thickness of the resulting PDMS layer was controlled to be around 3 nm for the pristine MEH-PPV films and less than 1 nm for the films of MEH-PPV/PS blends. Substrates of cover glass (premium cover glass, Fisherfinest) and SiOx wafer (thick silicon oxide coating *ca.* 500 nm grown on Si wafer) were also used for examining the effect arising from a built-in voltage at the substrate surface. After preparation, the samples were always protected in aluminum foil wrappings in an oxygen-free atmosphere before being tested. Some control samples were prepared in a glovebox (MBraun, Germany), but results were essentially identical to that prepared in ambient conditions.

To induce dewetting, the films were annealed in a vacuum oven at a temperature between 100 and 130 °C. Film morphology and the luminescence spectra were monitored and recorded. To minimize the effect of transient heating and cooling at the beginning and end of each annealing step, a number of simultaneously prepared identical samples were used for each dewetting experiment in which every sample was annealed exclusively for one annealing time. Optical microscopy and atomic force microscopy were used to visualize the film morphology.

PL Measurements and Sample Characterization. PL spectra were obtained with a fluorescence spectrometer (Perkin-Elmer). The dewetted film was also examined by utilizing a scanning near-field optical microscope for PL mapping. A confocal micro-PL optical system consisting of laser sources (473 and 632.8 nm), an inverted optical microscope (Olympus IX71), and a detector (Princeton Instrument, SP2300) in an optical circuit that integrated with an atomic force microscope (AFM) (Catalyst II, Bruker) served for probing the fluorescence property of small areas (*ca.* 1 μm^2) of

the samples. In order to explore the thickness of the residual monolayer of dewetted films, specular X-ray reflectivity measurements using synchrotron radiation (National Synchrotron Radiation Research Center, $\lambda = 0.154\,982$ nm) were employed. The resulting specular reflectivity curves were fitted to a multilayer model using the Abeles formulation.[43] The morphological information acquired by using AFM was used as guides for the fitting. The simulated curves fit well with the original data, as shown in Figure S1, and the fitting data in comparison to the results derived from AFM measurements are summarized in Table S1. From this fitting, the fine structure of the dewetted film was obtained.

Conflict of Interest: The authors declare no competing financial interest.

Acknowledgment. The authors sincerely thank Drs. C. T. Yuan and P. K. Wei of Academia Sinica of Taiwan for their contributions to, respectively, single-molecule spectroscopy and scanning near-field optical microscopy. We also appreciate the instructive discussions with the late Prof. Paul Barbara of University of Texas at Austin, USA, and Dr. Mark Geoghegan of University of Sheffield, UK. The work is supported by National Science Council of Taiwan (NSC 98-2120-M-007-010-; NSC 99-2120-M-007-005-; NSC 100-2120-M-007-002-; NSC 101-2221-E-007-040-MY3) and grants from the U.S. Air Force (AOARD-114055, -124064, -134026) under the U.S. Air Force-Taiwan NSC Nanoscience Initiatives.

Supporting Information Available: X-ray reflectivity measurements, PL spectra decomposition, and PL spectra of dewetting films. This material is available free of charge *via* the Internet at http://pubs.acs.org.

REFERENCES AND NOTES

1. Nguyen, T.-Q.; Doan, V.; Schwartz, B. J. Conjugated Polymer Aggregates in Solution: Control of Interchain Interactions. *J. Chem. Phys.* **1999**, *110*, 4068–4078.
2. He, G.; Li, Y.; Liu, J.; Yang, Y. Enhanced Electroluminescence Using Polystyrene As a Matrix. *Appl. Phys. Lett.* **2002**, *80*, 4247–4249.
3. Gustafsson, G.; Cao, Y.; Treacy, G. M.; Klavetter, F.; Colaneri, N.; Heeger, A. J. Flexible Light-Emitting Diodes Made from Soluble Conducting Polymers. *Nature* **1992**, *357*, 477–479.
4. Braun, D.; Heeger, A. J. Visible Light Emission from Semiconducting Polymer Diodes. *Appl. Phys. Lett.* **1991**, *58*, 1982–1984.
5. Berggren, M.; Inganas, O.; Gustafsson, G.; Rasmusson, J.; Andersson, M. R.; Hjertberg, T.; Wennerstrom, O. Light-Emitting Diodes with Variable Colours from Polymer Blends. *Nature* **1994**, *372*, 444–446.
6. Yu, J.; Hu, D.; Barbara, P. F. Unmasking Electronic Energy Transfer of Conjugated Polymers by Suppression of O_2 Quenching. *Science* **2000**, *289*, 1327–1330.
7. Tung, K.-P.; Chen, C.-C.; Lee, P.; Liu, Y.-W.; Hong, T.-M.; Hwang, K. C.; Hsu, J.-H.; White, J. D.; Yang, A. C.-M. Large Enhancements in Optoelectronic Efficiencies of Nano-Plastically Stressed Conjugated Polymer Strands. *ACS Nano* **2011**, *5*, 7296–7302.
8. Yan, M.; Rothberg, L. J.; Kwock, E. W.; Miller, T. M. Interchain Excitations in Conjugated Polymers. *Phys. Rev. Lett.* **1995**, *75*, 1992–1995.
9. An, Z.; Wu, C. Q.; Sun, X. Dynamics of Photogenerated Polarons in Conjugated Polymers. *Phys. Rev. Lett.* **2004**, *93*, 216407-1–216407-4.
10. Drori, T.; Gershman, E.; Sheng, C. X.; Eichen, Y.; Vardeny, Z. V.; Ehrenfreund, E. Illumination-Induced Metastable Polaron-Supporting State in Poly(p-Phenylene Vinylene) Films. *Phys. Rev. B* **2007**, *76*, 033203-1–033203-4.
11. Brédas, J.-L.; Norton, J. E.; Cornil, J.; Coropceanu, V. Molecular Understanding of Organic Solar Cells: The Challenges. *Acc. Chem. Res.* **2009**, *42*, 1691–1699.
12. Fox, M. *Optical Properties of Solids*; Oxford University Press: New York, 2001; Chapter 3 and Appendix D.
13. Inigo, A. R.; Chiu, H.-C.; Fann, W.; Huang, Y.-S.; Jen, U. S.; Hsu, C. H.; Peng, K.-Y.; Chen, S.-A. Structure and Charge Transport Properties in MEH-PPV. *Synth. Met.* **2003**, *139*, 581–584.
14. Feist, F. A.; Zickler, M. F.; Basché, T. Origin of the Red Sites and Energy Transfer Rates in Single MEH-PPV Chains at Low Temperature. *ChemPhysChem* **2011**, *12*, 1499–1508.
15. Becker, K.; Da Como, E.; Feldmann, J.; Scheliga, F.; Csanyi, E. T.; Tretiak, S.; Lupton, J. M. How Chromophore Shape Determines the Spectroscopy of Phenylene-Vinylenes: Origin of Spectral Broadening in the Absence of Aggregation. *J. Phys. Chem. B* **2008**, *112*, 4859–4864.
16. Schindler, F.; Lupton, J. M.; Feldmann, J.; Scherf, U. A Universal Picture of Chromophores in π-Conjugated Polymers Derived from Single-Molecule Spectroscopy. *Proc. Natl. Acad. Sci. U.S.A.* **2004**, *101*, 14695–14700.
17. Lin, H.; Tian, Y.; Zapadka, K.; Persson, G.; Thomsson, D.; Mirzov, O.; Larsson, P.-O.; Widengren, J.; Scheblykin, I. G. Fate of Excitations in Conjugated Polymers: Single-Molecule Spectroscopy Reveals Nonemissive "Dark" Regions in MEH-PPV Individual Chains. *Nano Lett.* **2009**, *9*, 4456–4461.
18. Bombardi, A. d. R.; Laureto, E.; Duarte, J. L.; da Silva, M. A. T.; Kias, I. F. L.; Patricio, P. S. O.; Silva, G. G.; Cury, L. A. Self-Organized MEH-PPV Domains in a TPU Matrix and the Consequences to the Luminescence Spectra. *J. Appl. Polym. Sci.* **2008**, *109*, 3659–3664.
19. Hu, D.; Yu, J.; Wong, K.; Bagchi, B.; Rossky, P. J.; Barbara, P. F. Collapse of Stiff Conjugated Polymers with Chemical Defects into Ordered, Cylindrical Conformations. *Nature* **2000**, *405*, 1030–1033.
20. Kim, D. Y.; Grey, J. K.; Barbara, P. F. A Detailed Single Molecule Spectroscopy Study of the Vibronic States and Energy Transfer Pathways of the Conjugated Polymer MEH-PPV. *Synth. Met.* **2006**, *156*, 336–345.
21. Köhler, A.; Hoffmann, S. T.; Bässler, H. An Order-Disorder Transition in the Conjugated Polymer MEH-PPV. *J. Am. Chem. Soc.* **2012**, *134*, 11594–11601.
22. Yu, P.; Ma, X. L.; Liu, C. C.; Tang, G.; Yang, A. C.-M. Dynamics of Exciton-Phonon Coupling Suppression in Conjugated Polymer MEH-PPV under Molecular Stresses by Time-Resolved Photoluminescence Spectroscopy, in preparation.
23. Vogelsang, J.; Adachi, T.; Brazard, J.; Vanden Bout, D. A.; Barbara, P. F. Self-Assembly of Highly Ordered Conjugated Polymer Aggregates with Long-Range Energy Transfer. *Nat. Mater.* **2011**, *10*, 942–946.
24. Vogelsang, J.; Brazard, J.; Adachi, T.; Bolinger, J. C.; Barbara, P. F. Watching the Annealing Process One Polymer Chain at a Time. *Angew. Chem., Int. Ed.* **2011**, *50*, 2257–2261.
25. Hagler, T. W.; Pakbaz, K.; Voss, K. F.; Heeger, A. J. Enhanced Order and Electronic Delocalization in Conjugated Polymers Oriented by Gel Processing in Polyethylene. *Phys. Rev. B* **1991**, *44*, 8652–8666.
26. Chan, N. Y.; Hao, X.-T.; Smith, T. A.; Dunstan, D. E. Conformational and Photophysical Changes in Conjugated Polymers Exposed to Couette Shear. *J. Phys. Chem. B* **2011**, *115*, 6838–6842.
27. Yang, G.; Li, Y.; Zhu, A.; White, J. O.; Drickamer, H. G. Effect of Controlled Streching on the Luminescence of Poly[2-methoxy-5-(2′-ethylhexoxy)-*p*-phenylenevinylene] in Dilute Solution in Poly(vinyl chloride) and Poly(vinyl acetate). *Macromolecules* **2000**, *33*, 3173–3175.
28. Chang, C.-H.; Chen, C.-C.; Yang, Y.-H.; Weng, Z.-M.; Liang J.-J.; Yang, A. C.-M. Optoelectronic Enhancement by Mechanical Stresses of Crystallizable Conjugated Polymer Poly(3-Hexylthiophene) Confined in Solid Films, submitted.
29. Onda, S.; Kobayashi, H.; Hatano, T.; Forumaki, S.; Habuchi, S.; Vacha, M. Complete Suppression of Blinking and Reduced Photobleaching in Single MEH-PPV Chains in Solution. *Phys. Chem. Lett.* **2011**, *2*, 2827–2831.
30. Kobayashi, H.; Tsuchiya, K.; Ogino, K.; Vacha, M. Spectral Multitude and Spectral Dynamics Reflect Changing Conjugation Length in Single Molecules of Oligophenylenevinylenes. *Phys. Chem. Chem. Phys.* **2012**, *14*, 10114–10118.
31. Schwartz, B. J. Conjugated Polymers as Molecular Materials: How Chain Conformation and Morphology Influence Energy Transfer and Interchain Interactions. *Annu. Rev. Phys. Chem.* **2003**, *54*, 141–172.
32. Shi, Y.; Liu, J.; Yang, Y. Device Performance and Polymer Morphology in Polymer Light Emitting Diodes: The

Control of Thin Film Morphology and Device Quantum Efficiency. *J. Appl. Phys.* **2000**, *87*, 4254–4263.
33. Reiter, G.; Hamieh, M.; Damman, P.; Sclavons, S.; Gabriele, S.; Vilmin, T.; Raphael, E. Residual Stresses in Thin Polymer Films Cause Rupture and Dominate Early Stages of Dewetting. *Nat. Mater.* **2005**, *4*, 754–758.
34. Yang, M. H.; Hou, S. Y.; Chang, Y. L.; Yang, A. C. M. Molecular Recoiling in Polymer Thin Film Dewetting. *Phys. Rev. Lett.* **2006**, *96*, 066105-1–066105-4.
35. Al Akhrass, S.; Reiter, G.; Hou, S. Y.; Yang, M. H.; Chang, Y. L.; Chang, F. C.; Wang, C. F.; Yang, A. C.-M. Viscoelastic Thin Polymer Films under Transient Residual Stresses: Two-Stage Dewetting on Soft Substrates. *Phys. Rev. Lett.* **2008**, *100*, 178301-1––178301-4.
36. Chang, Y. L. *Measurements and Analyses of Molecular Stresses, Packing, and Deformations in the Ultrathin Polymer Films Prepared by Spin Coating*. Master Thesis, National Tsing Hua University, Taiwan, 2008.
37. Chien, Y. *Thin Film Confinement-Induced Dewetting Instability, Photoluminescence Variation, and Young's Modulus Reduction in Ultrathin Polymer Films*. Master Thesis, National Tsing Hua University, Taiwan, 2011.
38. Heavens, O. S. *Optical Properties of Thin Films*; Butterworth: London, 1955.
39. Liu, J.; Guo, T.-F.; Yang, Y. Effects of Thermal Annealing on the Performance of Polymer Light Emitting Diodes. *J. Appl. Phys.* **2002**, *91*, 1595–1600.
40. Reiter, G. Dewetting of Thin Polymer Films. *Phys. Rev. Lett.* **1992**, *68*, 75–78.
41. de Gennes, P. G.; Brochard-Wyart, F.; Quéré, D. *Capillarity and Wetting Phenomena: Drops, Bubbles, Pearls, Waves*; Springer: New York, 2004.
42. Seemann, R.; Herminghaus, S.; Jacobs, K. Dewetting Patterns and Molecular Forces: A Reconciliation. *Phys. Rev. Lett.* **2001**, *86*, 5534–5537.
43. Nelson, A. Co-Refinement of Multiple-Contrast Neutron/X-Ray Reflectivity Data Using MOTOFIT. *J. Appl. Crystallogr.* **2006**, *39*, 273–276.
44. Bensimon, A.; Simon, A.; Chiffaudel, A.; Croquette, V.; Heslot, F.; Bensimon, D. Alignment and Sensitive Detection of DNA by a Moving Interface. *Science* **1994**, *265*, 2096–2098.
45. Sugimoto, T.; Habuchi, S.; Ogino, K.; Vacha, M. Conformation-Related Exciton Localization and Charge-Pair Formation in Polythiophenes: Ensemble and Single-Molecule Study. *J. Phys. Chem. B* **2009**, *113*, 12220–12226.
46. Becker, K.; Lagoudakis, P. G.; Gaefke, G.; Hoger, S.; Lupton, J. M. Exciton Accumulation in π-Conjugated Wires Encapsulated by Light-Harvesting Macrocycles. *Angew. Chem., Int. Ed.* **2007**, *46*, 3450–3455.
47. Thomsson, D.; Camacho, R.; Tian, Y.; Yadav, D.; Sforazzini, G.; Anderson, H. L.; Scheblykin, I. G. Cyclodextrin Insulation Prevents Static Quenching of Conjugated Polymer Fluorescence at the Single Molecule Level. *Small* **2013**, 10.1002/smll.201203272.